

1 **The Effect of Dynamic Loading on the Shear Strength of Pyroclastic Ash Deposits and Implications**
2 **for Landslide Hazard: The Case of Pudahuel Ignimbrite, Chile**

3
4 Sergio A. Sepúlveda¹, David N. Petley^{2,3}, Matthew J. Brain², Neil Tunstall²

5
6 ¹: Departamento de Geología, Universidad de Chile. Plaza Ercilla 803, Santiago, Chile. Phone +56-2-
7 29784102, e-mail: sesepulv@ing.uchile.cl

8 ²: Department of Geography and Institute of Hazard, Risk and Resilience, Durham University, South
9 Road, Durham DH1 3LE, United Kingdom.

10 ³: Present address: School of Environmental Sciences, University of East Anglia, Norwich, N4TJ R7
11 United Kingdom.

12
13 **Abstract**

14 The co-seismic and post-seismic behaviour of pyroclastic ash deposits and its influence on slope
15 stability remains as a challenging subject in engineering geology. Case studies in volcanic areas of the
16 world suggest that soil structural changes caused by seismic shaking results in landslide activity. It is
17 critical to constrain how this kind of soil behaves during coseismic ground shaking, as well as the
18 effects of dynamic loading on shear strength parameters after shaking. Direct shear tests carried out
19 on cineritic volcanic materials from the Pudahuel Ignimbrite Formation in central Chile show a direct
20 effect of cyclic loading on the shear strength and in a minor extent on the rheology. A high apparent
21 cohesion found in monotonic shear tests, likely attributed to suction and cementation, is destroyed
22 by dynamic loading. At the same time, the internal friction angle rises. This defines a differential
23 post-dynamic behaviour depending on normal effective stress conditions, which favour the
24 occurrence of shallow landslides. These results show how the use of shear strength parameters
25 obtained from standard monotonic direct shear tests may produce misleading results when
26 analyzing seismic slope stability in this type of soils.

27

28 **1. Introduction**

29

30 Pyroclastic ash deposits are widely distributed in volcanic regions, presenting complex and
31 differential geotechnical behaviour during earthquakes. While they tend to be competent
32 foundation soils in aseismic conditions, their behaviour during seismically-induced dynamic loading
33 can be problematic. For example, in central Chile Pleistocene, volcanic deposits are widespread and
34 were associated with higher levels of damage in buildings during the 1985 (Mw 7.8) Valparaiso and
35 the 2010 (Mw 8.8) megathrust earthquakes (Leyton et al., 2011, 2013). Studies of the geotechnical
36 behaviour of these types of soils have shown that they are characterized by high shear strengths
37 (cohesion up to 90 kPa and friction angles of 35°-40° in unsaturated samples), with an important
38 component of cohesion due to the presence of weak cements and/or negative pore pressures (i.e.
39 apparent cohesion), which may be destroyed by saturation or seismic shaking (e.g. Bommer et al.,
40 2002; Rolo et al., 2004 and references therein). In addition, when saturated they can be susceptible
41 to liquefaction (e.g. Gratchev and Towhata, 2010). Such soils have proved to be highly prone to
42 earthquake-induced landslides, with documented examples from a variety of locations, including
43 Central America (Evans and Bent, 2002), Japan (Gratchev and Towhata, 2010; Chigira et al., 2013)
44 and Patagonia (Sepúlveda et al. 2010).

45

46 Given the widespread occurrence in different seismogenic settings and susceptibility to failure of
47 pyroclastic hillslope deposits, it is critical to constrain how they behave during coseismic ground
48 shaking, as well as the effects of dynamic loading on soil structural change and hence shear strength
49 parameters due to precursory seismic events. However, this has been challenging due to the
50 difficulties in generating representative dynamic stress conditions under laboratory conditions (e.g.
51 Bray and Travararou, 2007; Wasowski et al., 2011). In a slope, seismic loading generates both
52 dynamic normal and shear stresses, which has conventionally proven to be difficult to reproduce

53 experimentally. However, recent technological advances and experimental work have led to
54 significant advances in our understanding of coseismic strain accumulation in hillslopes (e.g. Schulz
55 and Wang, 2014; Brain et al., 2015).

56

57 In this paper we present the results of a programme of geotechnical tests undertaken to analyse the
58 dynamic and post-dynamic behaviour of pyroclastic ash deposits from the Pudahuel Ignimbrite
59 Formation in central Chile (Fig. 1). This formation was observed to be associated with both local site
60 effects and earthquake-induced landslides during large subduction earthquakes in 1985 and 2010
61 (Leyton et al., 2011; Sepúlveda et al., 2015). In this study we have utilised a dynamic back pressured
62 shear box (DynBPS) that is able to replicate dynamic normal and shear stress states in slopes under
63 laboratory test conditions.

64

65

66 **2. Materials & Methods**

67

68 **2.1 The Pudahuel Ignimbrite deposits**

69

70 The Pudahuel Ignimbrite is an Upper Pleistocene stratigraphic unit mainly composed of pyroclastic
71 ash deposits, widely distributed in the valleys of Maipo and Cachapoal rivers in central Chile (Fig. 1)
72 as well as the Yaucha and Papagayos rivers in Argentina. It corresponds to deposits interpreted to
73 originate from a single huge, violent eruption, or a series of closely spaced eruptions dated at
74 $450,000 \pm 60,000$ years B.P. (Stern et al., 1984), from the Maipo volcanic complex (Diamante
75 Caldera, Fig. 1) located on the border of Chile and Argentina at $34^{\circ}\text{S } 10^{\circ}\text{W}$. The unit is defined in the
76 district of Pudahuel in western Santiago (Maipo valley, Fig. 1), where rhyolitic pumice and ash tuff
77 deposits are found in the upper 10 to 40 m (Wall et al., 1999; Wall, 2000; Rebolledo et al., 2006). The
78 deposits have been described as a basal ash fall layer overlain by a thick (>30 m) pyroclastic ash flow

79 and a <5 m thick uppermost pyroclastic surge (Rebolledo et al., 2006). The water table in Pudahuel is
80 found at c. 14 m depth, indicating that part of the deposit is saturated. Petrographic and
81 geochemical analyses by Stern et al. (1984) showed that similar deposits in a hilly area known as
82 Tierras Blancas (“white land”) near the town of Machalí in the Cachapoal valley (Fig. 1) and other
83 places downstream correspond to the same deposit. The total volume for the pyroclastic flows was
84 estimated to be 450 km³ (Stern et al., 1984).

85

86 **2.2 Sample collection and lithological characterisation**

87

88 In this study, undisturbed block samples (e.g. ASTM D7015) were collected from Machalí (Tierras
89 Blancas) and Pudahuel deposits (Fig. 1) in Chile and transported to UK for testing in appropriate
90 protected conditions to prevent disturbance and desiccation. Both samples can be described as
91 whitish volcanic ash with pumice fragments and occasional lithics. The soil in-situ is dry, with
92 moisture contents below 5 %. The soil bulk density at natural moisture content is close to 1 g/cm³.
93 Whilst it is able to form stable steep cuts and even unsupported caves and small tunnels in Machalí
94 (Fig. 1), it shows very friable behaviour. Grain size analyses undertaken by sieving and laser
95 granulometry (Fig. 2) show that in both cases the dominant grain size is sand, with 10 - 20% of silt
96 and very little clay (< 1%). The soil is slightly coarser at Pudahuel, but in both cases the amount of
97 gravel is less than 5%, mainly resulting from the presence of gravel-sized pumice fragments.

98

99 **2.3 Testing Equipment**

100

101 Direct shear strength tests were carried out at the Laithwaite Landslide Laboratory at Durham
102 University in the UK. In this study we use two direct shear testing machines, both manufactured by
103 GDS Instruments in the UK. Firstly, to undertake standard monotonic direct shear tests, we used a
104 Back-Pressured Shear Box (BPS). Secondly, to assess dynamic behaviour we used the new Dynamic

105 Back-Pressured Shear Box (DynBPS). The machines are located in a climate-controlled laboratory
106 that regulates both temperature ($\pm 1^\circ\text{C}$) and relative humidity ($\pm 1\%$). Both machines subject
107 samples with plan dimensions of 100×100 mm and a height of 20 mm to direct shear, which we
108 consider to be the most representative of landslide rupture in our field settings. Experiments can be
109 undertaken in either a dry or a saturated state. The sample is situated in a water bath within a
110 sealed pressure vessel. If the test is to be undertaken in dry conditions the water bath is left dry. If
111 the test is to be undertaken under saturated conditions the water bath is filled and pressurised,
112 allowing the pore water pressure to be measured and controlled via a pressure controller.

113 In the BPS, as with a conventional direct shear machine, the normal stress is applied via a vertical
114 ram acting on the full cross-section of the sample. In this case the applied force, which is applied via
115 a piston regulated by a pressure controller, is measured with a load cell. Deformation is measured
116 via LVDT. The apparatus permits deformation under stress (or load), or strain (displacement) control.
117 In conjunction with the pressure controller for the water bath and a pore pressure transducer, it is
118 possible to control effective normal stress. Shear stress is applied as per a conventional direct shear
119 machine, in this case via a stepper motor. The applied load is measured with a load cell, permitting
120 control of stress, load, displacement or strain. The maximum allowed shear displacement is 20 mm.

121 In the DynBPS machine, both vertical and shear stress can be applied under dynamic conditions up
122 to 5 Hz. Dynamic load can be controlled in terms of displacement or stress; the dynamic vertical and
123 horizontal loads are applied separately. More details on the testing equipment are provided by Brain
124 et al. (2015).

125 **2.3 Laboratory Testing Programme**

126 In this series of experiments, the undisturbed block samples were carefully sub-sampled to the
127 dimensions of the testing cell in preparation for laboratory testing. Samples with gravel-size pumice
128 fragments were excluded for testing. The majority of tests for Machalí samples were undertaken in

129 an unsaturated state, replicating the observed conditions at the site. In contrast, for the Pudahuel
130 samples, and a small number of the Machalí samples, saturated tests were undertaken.

131 A total of 21 experiments on undisturbed samples, and 12 experiments on remoulded samples, were
132 undertaken (Tables 1 and 2, Figs. 3, 4 and 5). In the case of the Machalí undisturbed samples, these
133 consisted of ten monotonic and five dynamic tests. For the Pudahuel samples, three monotonic and
134 three dynamic tests were performed on undisturbed samples. In addition, a series of three
135 monotonic and three dynamic tests on remoulded samples were undertaken for each site. The
136 results can be compared with shear strength tests that had been previously undertaken by Lagos
137 (2003) and Rebolledo et al. (2006) on the same material, including several monotonic direct shear
138 tests on remoulded samples from a range of sites and one consolidated isotropic undrained (CIU)
139 triaxial test series in an undisturbed sample from Pudahuel.

140 To obtain the shear strength failure envelopes, a series of monotonic direct shear tests were
141 undertaken on undisturbed and remoulded samples from Machalí under both unsaturated and
142 saturated conditions, and under saturated conditions for the Pudahuel samples, according to local
143 site conditions (Table 1). In these tests the samples were consolidated to a predetermined normal
144 total (and, in the case of the saturated samples, effective) stress, and then sheared at a constant
145 displacement rate of 0.1 mm/min in fully drained conditions. During testing, measurements were
146 made of normal stress and strain, and shear stress and strain. In the case of the saturated tests, the
147 pore water pressure was also recorded to permit calculation of normal effective stress.

148 The aim of the dynamic tests was not to generate failure under dynamic conditions. The imposed
149 stresses during the dynamic phases of the tests were designed to keep the stress path below the
150 static failure envelope. In each case the aim was to investigate whether dynamic testing that did not
151 cause sample failure had an impact on monotonic behaviour. Thus, after dynamic loading the
152 samples were taken under monotonic loading conditions (i.e. through conventional direct shear)

153 until displacement reached full travel. As such these experiments allow studying the role of dynamic
154 loading in preparing slopes for failure rather than inducing failure itself during dynamic loading.

155 The dynamic tests (see Table 2) were undertaken in four stages:

156 • In Stage 1, the samples were consolidated to predetermined normal effective stresses,
157 replicating the depth range of potential shear surfaces in Machalí estimated from field
158 observations (1 to 20 m). The normal effective stresses applied for the Machalí samples
159 were of 50, 100, 150 and 200 kPa. For the Pudahuel test series we opted to investigate the
160 influence of different dynamic loads at the same normal stress. In this case, all dynamic tests
161 were carried out at an effective normal stress of 150 kPa to represent stress conditions
162 below the water table in Pudahuel.

163 • Stage 2 consisted of the application of a monotonic shear stress at a displacement rate of 0.1
164 mm/min until a predetermined shear stress of 50 % the normal stress was achieved (Table
165 2), which replicated the stress state encountered in typical slopes at the Machalí site. The
166 same stress conditions were applied to the Pudahuel samples to allow comparison.

167 • In Stage 3 cyclic stresses were applied for 30 cycles at a frequency of 2 Hz. This is the
168 dominating natural frequency measured using H/V or Nakamura's method (Leyton et al.
169 2011) at a site at Pudahuel. For simplicity, in-phase horizontal and normal loads were
170 applied, with maximum horizontal stress amplitude (K_h) being double the vertical stress (K_v).
171 During the 2010 earthquake, the only record for these soils (Maipú seismic station in
172 Pudahuel deposits) recorded peak accelerations of 0.54 g (horizontal) and 0.23 g (vertical)
173 (Saragoni & Ruiz, 2012). For the Machalí test series on unsaturated samples, the loads were
174 selected such that the horizontal load was around 50 % of the shear strength at the applied
175 normal stress. The peak horizontal cyclic shear stresses applied were of 52, 75, 98 and 120
176 kPa, respectively. For the tests on saturated samples from the Pudahuel site, all taken at a
177 normal effective stress of 150 kPa and an initial shear stress of 75 kPa, the applied peak

178 horizontal shear stresses were of 50, 100 and 200 kPa, with an in-phase vertical load half the
179 horizontal load (Table 2). For comparison, a similar test on a saturated sample from Machalí
180 was carried out at the same stress state, with a peak cyclic horizontal stress of 100 kPa.

- 181 • The fourth and last stage was carried out after the cyclic loading had been completed. Then,
182 the sample was loaded monotonically to full travel at the initial normal effective stress,
183 allowing recording of post-dynamic peak and residual strength and obtaining the
184 corresponding failure envelopes.

185

186 **3. Test Results**

187

188 **3.1 Monotonic tests**

189

190 The results of monotonic tests are summarized in Table 1. The Machalí undisturbed samples show a
191 high cohesion of slightly over 60 kPa under unsaturated conditions, which is reduced to 17 kPa when
192 the sample is saturated, suggesting that this is predominantly an apparent cohesion effect. The peak
193 friction angle varies between 39° and 51°, being higher for saturated samples, suggesting a sample
194 densification caused by cohesion loss. The monotonic tests on remoulded samples show smaller
195 cohesion values (c. 8 kPa) but similar friction angles (47°) to the undisturbed samples. Residual
196 strength is generally similar to peak strength in relation to the friction angle, but in the remoulded
197 samples all cohesion is lost.

198

199 While the (apparent) cohesion is quite variable from one site to another and it is dependent on the
200 saturation conditions, the friction angle is comparable with those obtained from standard direct
201 shear tests in both unsaturated and saturated samples from different sites by Rebolledo et al.
202 (2006), which range from 38° to 47°. The peak cohesion obtained by these authors varied from 7 to
203 20 kPa.

204

205 The undisturbed, unsaturated samples tend to show a semi-ductile rheology (Fig. 3), while the
206 undisturbed-saturated and remoulded-unsaturated samples show a more variable behaviour from
207 brittle-ductile to semi-ductile curves.

208

209 **3.2 Dynamic test results**

210 **3.2.1 Machalí**

211

212 Results of dynamic tests on unsaturated, undisturbed Machalí samples are summarized in Fig. 4. In
213 all cases the dynamic stresses did not cause the stress path to cross the monotonic failure envelope.
214 During the cyclic loading shear displacements between 2.8 and 4.5 mm were recorded, most of
215 which registered during the first ten cycles (Fig. 4). At the same time, the shear stresses increased
216 with each cycle (Fig. 3b), suggesting a strain-hardening response during cyclic loading.

217

218 In most cases the samples showed a clear post-dynamic peak strength with a post-peak strain-
219 softening to semi-ductile behaviour (Fig. 3b), with residual values between 80 % and 95 % of the
220 peak value. If linear envelopes are traced through the peak and residual values (Fig. 4), the resulting
221 post-dynamic strength parameters are zero cohesion and friction angles of 55° (peak) and 51°
222 (residual). The experiment was repeated on remoulded samples under the same loading conditions.
223 In this case the results were essentially identical, with no cohesion and friction angles of 56° (peak)
224 and 52° (residual) for the post-dynamic failure envelopes.

225

226 **3.2.2 Pudahuel**

227

228 In this series of tests on saturated samples, the effect of changes on the cyclic load amplitude was
229 investigated. In all cases except one (the remoulded sample with a 200 kPa peak horizontal stress)

230 the dynamic stresses did not cross the monotonic failure envelope. Similarly as for the other tests,
231 monotonic shear under displacement control was applied afterwards until the apparatus reached
232 full travel.

233

234 In these tests, excess pore water pressures developed during the dynamic phase, although these
235 were less than 10% of the back pressure and quickly dissipated. The post-dynamic peak shear
236 strengths were all 'above' the monotonic failure envelope observed for the saturated Pudahuel
237 samples, showing an increase in strength with higher loading amplitude for undisturbed samples,
238 and a more variable behaviour for the remoulded samples (Fig. 4c). The strength of the Pudahuel
239 sample is higher than the undisturbed, saturated Machalí sample tested under the same loading
240 conditions, which is consistent with the monotonic test results. In turn, the Machalí saturated
241 sample shows a slightly higher strength than the unsaturated test at the same dynamic loading
242 conditions.

243

244 **4. Discussion**

245

246 Figure 5 presents the dynamic and static failure envelopes measured for the Machalí series of tests.
247 The monotonic unsaturated failure envelope displays a high level of cohesion, which we interpret as
248 cohesion generated by suction (i.e. apparent cohesion) and inter-particle bonding. When tested
249 under saturated, monotonic conditions the samples lose almost all of their cohesion but display a
250 higher level of internal friction than for unsaturated conditions. Remoulded samples tested under
251 unsaturated conditions show essentially identical strength parameters to the saturated undisturbed
252 samples (Fig. 5), suggesting that the behaviour of the undisturbed unsaturated samples,
253 characterized by high cohesion, is dominated by the effects of suction. There is still some cohesion in
254 saturated samples that can be attributed to weak cements, which are destroyed during cyclic
255 loading. Preliminary X-ray diffraction analyses carried out at the University of Chile (Morata, pers.

256 comm., 2014) show the presence of clay minerals and silica polymorphs. Cementation due to
257 chemical weathering producing clay and silica viscous agents is likely in the Pudahuel Ignimbrite
258 soils. The effect of loss of suction and/or destruction of cementation in pyroclastic materials has
259 been proposed as mechanism of strength loss in seismically-induced landslides in volcanic soils
260 (Evans et al., 2002). As found in similar volcanic soils elsewhere (Rolo et al. 2002 and references
261 therein), the effect of such cements and suction may explain the metastable behaviour of these soils
262 that can sustain steep slopes and caves in static conditions but tend to fail during heavy rainfall or
263 seismic shaking, or show poor behaviour as foundation soil during earthquakes (Leyton et al. 2011).

264

265 The samples subject to dynamic testing show no cohesion, but have a higher angle of internal
266 friction (Fig. 5). It appears that the dynamic loading cause a restructuring of the sample that
267 destroys (apparent) cohesion (i.e. results in a loss of suction and cementation) but increases the
268 angle of internal friction, perhaps due to some densification or strain hardening effect. Additionally,
269 the rheology tends to be more brittle, or displaying evidence of strain softening, after shaking. The
270 results from the Pudahuel site also show an increase in shearing resistance for higher shear stresses
271 (Fig. 4).

272

273 Given the nature of the climate in the study area, it is likely that seismic shaking usually occurs when
274 slopes are in an unsaturated state. Thus, the loss of cohesion as a result of dynamic loading is an
275 important effect. In studied soils, for potential shallow landslides, this loss of cohesion will increase
276 the potential for instability, and these effects will not be compensated by the higher angle of
277 internal friction. For deeper landslides (shear surfaces with normal stress over c. 100 kPa, where the
278 failure envelopes in Fig. 5 intersect) the loss of cohesion is likely to be less important, with shear
279 strength being dominated by the higher angle of internal friction (Fig. 5).

280

281 For example, a simple stability analysis of a theoretical 2D, unsaturated soil slope of 30 degrees
282 using the infinite slope method (e.g. Das, 1998) with the shear strength parameters of the
283 undisturbed, unsaturated Machalí samples for both monotonic and post-dynamic conditions show
284 how for shallow slides the loss of cohesion reduces the static factor of safety in over 40%, while for
285 deeper slides, where the increase of friction angle dominates the behaviour, the static factor of
286 safety may even increase despite the cohesion loss (Table 3). Thus, the behaviour observed in this
287 test series suggests that in these materials seismic shaking is likely to promote shallow rather than
288 deep-seated landslides, which is in accordance with observed behaviour during the 2010 earthquake
289 (Sepúlveda et al. 2012, 2015).

290

291 The results illustrate the effects of dynamic loading during earthquakes on pyroclastic ash soils and
292 hence possible changes in shear strength parameters due to precursory seismic events that may
293 modify the stability conditions of slopes. The effect of loading frequencies or horizontal to vertical
294 stress ratios in such changes need to be further investigated, as well the role of liquefaction on slope
295 failures in these types of soil.

296

297 **5. Conclusions**

298

299 Direct shear tests carried out on pyroclastic materials from the Pudahuel Ignimbrite Formation in
300 central Chile show a direct effect of cyclic loading on the shear strength, and in a minor extent on
301 the rheology. A high apparent cohesion found in monotonic shear tests, likely attributed to suction
302 and cementation, is destroyed by dynamic loading. At the same time, the internal friction angle
303 rises. This defines a differential behaviour with a post-dynamic shear strength lower than the static
304 strength at normal effective stresses below 100 kPa, due to loss of cohesion, while for higher normal
305 stresses the effect of frictional resistance results in higher strength. Additionally, if higher shear
306 stresses are applied for a given normal stress, the peak strength increases. The results are consistent

307 with observations of differential behaviour as foundation soils and shallow landsliding in slopes of
308 the Pudahuel Ignimbrite Formation during recent strong earthquakes in the region. We conclude
309 that seismic shaking in this kind of cineritic soils induce changes in shear strength leading to shallow
310 slope failures and that the use of shear strength from monotonic direct shear tests may produce
311 quite misleading results when studying seismic slope stability in this type of soils.

312 **Acknowledgements**

313 The authors acknowledge the support of the Durham International Fellowships for Research and
314 Enterprise (DIFeREns, COFUNDED by Durham University and the European Union), for funding a
315 research stay of Dr. Sepulveda at the Institute of Hazard, Risk and Resilience of Durham University,
316 where the laboratory testing for this work was carried out. Many thanks to A. Alfaro and O. González
317 who aided with the sampling and C. Longley who collaborated with the geotechnical index tests.

318 **References**

319 Bommer, J.J., Rolo, R., Mitoulia, A., Berdousis, P., 2002. Geotechnical properties and seismic slope
320 stability of volcanic soils: 12th European Conference on Earthquake Engineering, London, paper 695,
321 10 p.

322 Brain, M.J., Rosser, N.J., Sutton, J., Snelling, K., Tunstall, N., Petley, D.N., 2015. The effects of normal
323 and shear stress wave phasing on coseismic landslide displacement. *Journal of Geophysical*
324 *Research-Earth Surface*, 120, 1009-1022.

325 Bray, J., Travasarou, T., 2007. Simplified procedure for estimating earthquake-induced deviatoric
326 slope displacements. *Journal of Geotechnical and Geoenvironmental Engineering* 133(4), 381-392.

327 Chigira, M., Nakasuji, A., Fujiwara, S., Sakagami, M., 2013. Catastrophic landslides of pyroclastics
328 induced by the 2011 off the Pacific Coast of Tohoku Earthquake. In: Ugai, K., Yagi, H., Wakai, A.
329 (eds.). *Proceedings of the International Symposium on Earthquake-induced Landslides*, Kiryu, Japan,
330 2012, pp. 139-147.

331 Das, B.M., 1998. Principles of Geotechnical Engineering. Fourth Edition, PWS Publishing Company,
332 Boston.

333 Evans, S.G., Bent, A.L., 2002. The Las Colinas landslide, Santa Tecla: A highly destructive flowslide
334 triggered by the January 13, 2001, El Salvador earthquake. In: Rose, W.I. et al. (Eds.), Natural Hazards
335 in El Salvador. Geological Society of America Special Paper 375, pp. 25-37.

336 Gratchev, I., Towhata, I., 2010. Geotechnical characteristics of volcanic soil from seismically induced
337 Aratozawa landslide, Japan. Landslides 7, 503-510.

338 Lagos, J., 2003. Pudahuel Ignimbrite: geological and geotechnical characterization for its seismic
339 response. Degree dissertation, Department of Geology, Universidad de Chile (in Spanish).

340 Leyton, F., Sepúlveda S.A., Astroza, M., Rebolledo, S., Acevedo, P., Ruiz, S., González, L., Foncea, C.,
341 2011. Seismic zonation of the Santiago basin, Chile. Proceedings, 5th International Conference on
342 Earthquake Geotechnical Engineering, Santiago, Chile, paper 5.6.

343 Leyton, F., Ruiz, S., Sepúlveda, S.A, Contreras, J.P., Rebolledo, S., Astroza, M., 2013. Microtremors'
344 HVSR and its correlation with surface geology and damage observed after the 2010 Maule
345 earthquake (Mw 8.8) at Talca and Curicó, Central Chile. Engineering Geology 161, 26-33.

346 Rebolledo, S., Lagos, J., Verdugo, R., Lara, M., 2006. Geological and geotechnical characteristics of
347 the Pudahuel ignimbrite, Santiago, Chile. Proceedings, International Association of Engineering
348 Geology and the Environment X Congress, Nottingham. The Geological Society of London, paper 106.

349 Rolo, R., Bommer, J.J., Houghton, B.F., Vallance, J.W., Berdousis, P., Mavrommati, C., Murphy, W.,
350 2004. Geologic and engineering characterization of Tierra Blanca pyroclastic ash deposits. In: Rose,
351 W.I. et al. (Eds.), Natural Hazards in El Salvador. Geological Society of America Special Paper 375,
352 pp.55-67

353 Saragoni, R., Ruiz, S., 2012. Implicaciones y nuevos desafíos de diseño sísmico de los acelerogramas
354 del terremoto de 2010. In: Mw=8.8 Terremoto en Chile, 27 de febrero 2010, Departamento de
355 Ingeniería Civil, Universidad de Chile, 127-146.

356 Schulz, W. H., and G. Wang (2014), Residual shear strength variability as a primary control on
357 movement of landslides reactivated by earthquake-induced ground motion: Implications for coastal
358 Oregon, U.S., *Journal of Geophysical Research Earth Surface*, 119, 1617–1635, Sepúlveda, S.A., Serey,
359 A., Lara, M., Pavez, A., Rebolledo, S., 2010. Landslides induced by the April 2007 Aysén Fjord
360 earthquake, Chilean Patagonia. *Landslides* 7, 483-492.

361 Sepúlveda S.A., Petley, D.N., Tunstall, N., 2015. Shear strength changes due to saturation and cyclic
362 loading in the “Tierras Blancas” pyroclastic soils, Machalí, Central Chile. Proceedings, XI Chilean
363 Seismology and Seismic Engineering Congress, Santiago, paper 64.

364 Stern, C.R., Amini, H., Charrier, R., Godoy, E., Hervé, F., Varela, J., 1984. Petrochemistry and age of
365 rhyolitic pyroclastic flows which occur along the drainage valleys of Río Maipo and Río Cachapoal
366 (Chile) and the Río Yaucha and Río Papagayos (Argentina). *Revista Geológica de Chile* 23, 39-52.

367 Wall, R., Sellés, D., Gana, P. 1999. Hoja Tiltil-Santiago, Región Metropolitana. Serie Mapas Geológicos
368 (11), Servicio Nacional de Geología y Minería, Santiago.

369 Wall, R. 2000. La ignimbrita Pudahuel (Chile Central, 33.5-34°S): nuevos antecedentes. Proceedings,
370 Chilean Geological Congress, v.2, 88-89.

371 Wasowski, J., Keefer, D.K., Lee, C.-T. 2011. Toward the next generation of research on earthquake-
372 induced landslides: Current issues and future challenges. *Engineering Geology*, 122(1–2), 1-8.

373

374 **TABLES**

375

376 Table 1. Monotonic shear tests settings and resulting shear strength parameters (peak and residual

377 strength) on Machalí and Pudahuel sites.

378

Site	Sample Condition	Saturation	Normal Effective Stresses (kPa)	Peak Cohesion (kPa)	Peak Friction Angle (°)	Residual Cohesion (kPa)	Residual Friction Angle (°)
<i>Machalí</i>	Undisturbed	Unsaturated	50, 100, 150, 200, 350	64.2	39.4	62.7	37.3
<i>Machalí</i>	Undisturbed	Saturated	35, 70, 100, 140, 200	17.0	46.4	6.1	47.0
<i>Machalí</i>	Remoulded	Unsaturated	50, 150, 200	8.6	47.4	0.0	44.2
<i>Pudahuel</i>	Undisturbed	Saturated	70, 150, 250	13.7	51.3	12.1	44.8
<i>Pudahuel</i>	Remoulded	Saturated	70, 150, 250	0.0	50.9	0.0	51.6

379

380

381

382

383

384 Table 2. Summary of dynamic test settings for Machalí and Pudahuel samples.

385

Sample Site	Sample condition	Saturation	Normal Effective Stress (kPa)	Initial Shear Stress (kPa)	Max. Horizontal Cyclic Stress, Kh (kPa)	Max. Vertical Cyclic Stress, Kv (kPa)
<i>Machalí</i>	Undisturbed	Unsaturated	50	25	52	26
<i>Machalí</i>	Undisturbed	Unsaturated	100	50	75	37
<i>Machalí</i>	Undisturbed	Unsaturated	150	75	98	49
<i>Machalí</i>	Undisturbed	Unsaturated	200	100	120	60
<i>Machalí</i>	Undisturbed	Saturated	150	75	100	50
<i>Machalí</i>	Remoulded	Unsaturated	50	25	75	37
<i>Machalí</i>	Remoulded	Unsaturated	150	75	98	49
<i>Machalí</i>	Remoulded	Unsaturated	200	100	120	60
<i>Pudahuel</i>	Undisturbed	Saturated	150	75	50	25
<i>Pudahuel</i>	Undisturbed	Saturated	150	75	100	50
<i>Pudahuel</i>	Undisturbed	Saturated	150	75	200	100
<i>Pudahuel</i>	Remoulded	Saturated	150	75	50	25
<i>Pudahuel</i>	Remoulded	Saturated	150	75	100	50
<i>Pudahuel</i>	Remoulded	Saturated	150	75	200	100

386

387

388

389

390 Table 3. Results of static slope stability analyses using the infinite slope method for unsaturated soils
391 without seepage using monotonic and post-dynamic strength parameters for Machalí undisturbed
392 samples. A slope angle of 30 degrees is assumed.

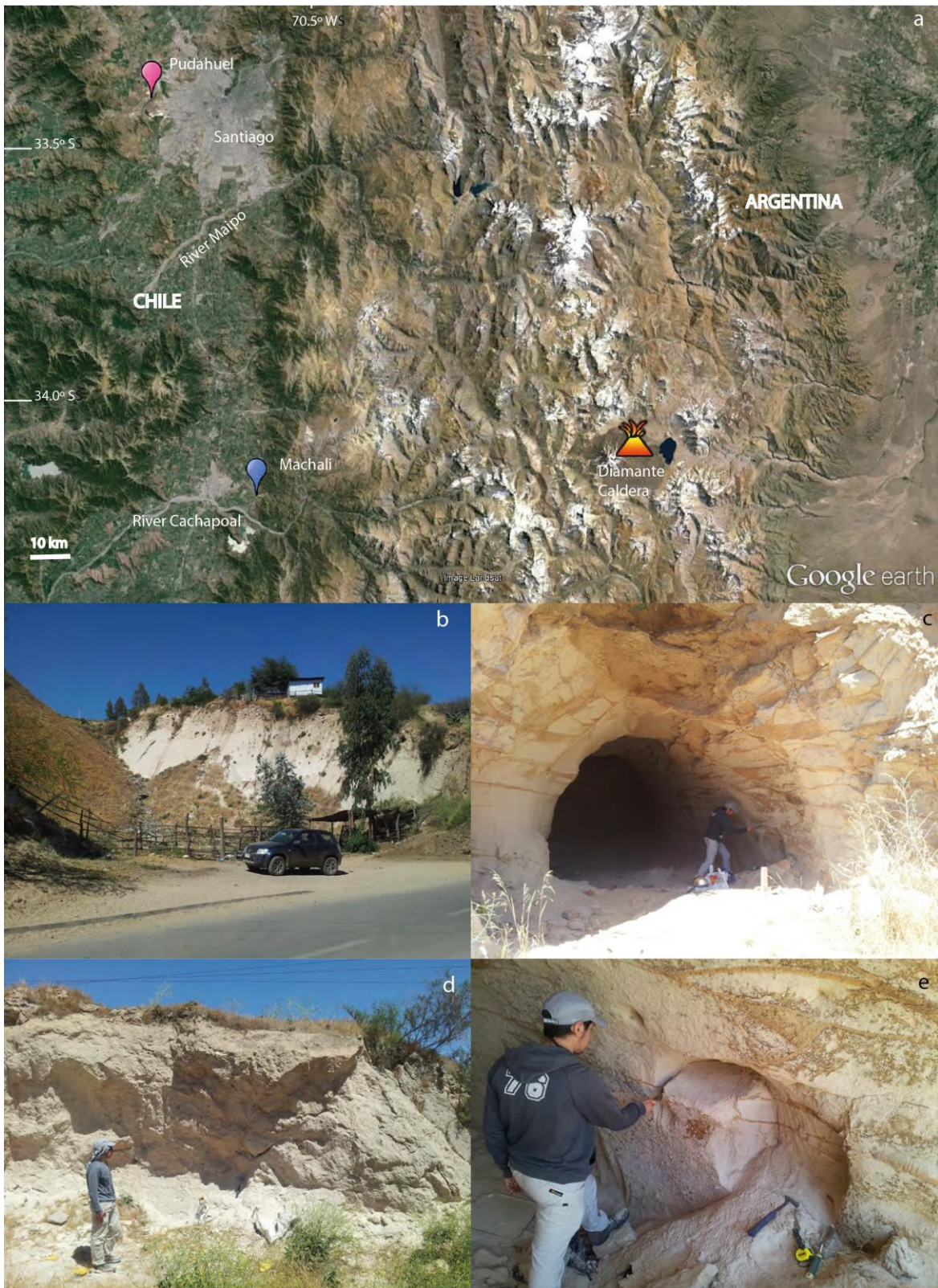
393

<i>Strength parameters</i>	<i>Factor of Safety, depth 5 m</i>	<i>Factor of Safety, depth 30 m</i>
Monotonic (c=64kPa, $\phi=39^\circ$)	4.3	1.9
Post-dynamic (c=0kPa, $\phi=55^\circ$)	2.5	2.5

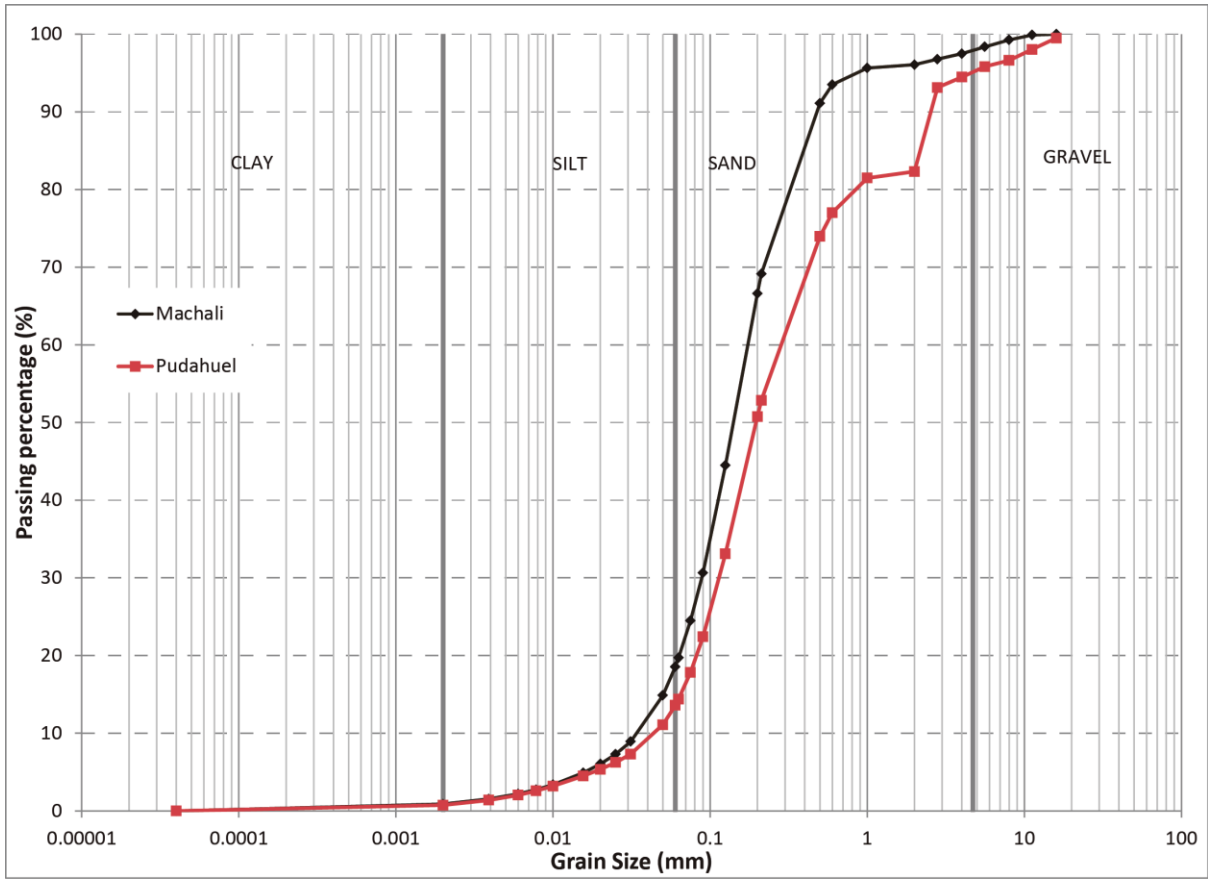
394

395

396

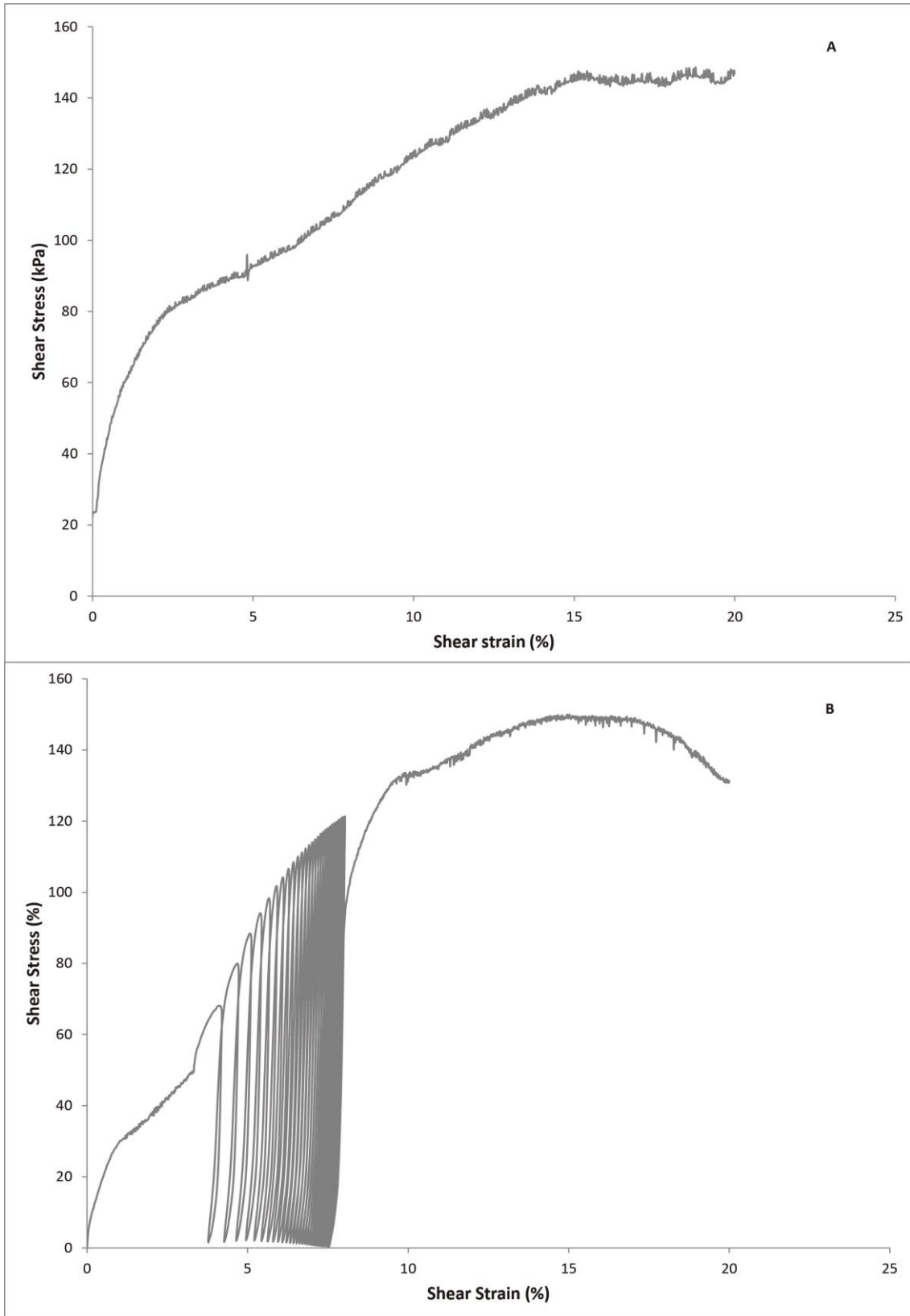


398
399 Figure 1. a) Landsat-Google Earth image indicating the location of Pudahuel ignimbrite sampling sites
400 of Pudahuel (pink symbol) and Machali (blue symbol) and Diamante Caldera; b) Shallow landslide in
401 Machali; c) Machali samples site in unsupported cave; d) Pudahuel samples site; e) Detail of sample
402 carving process.



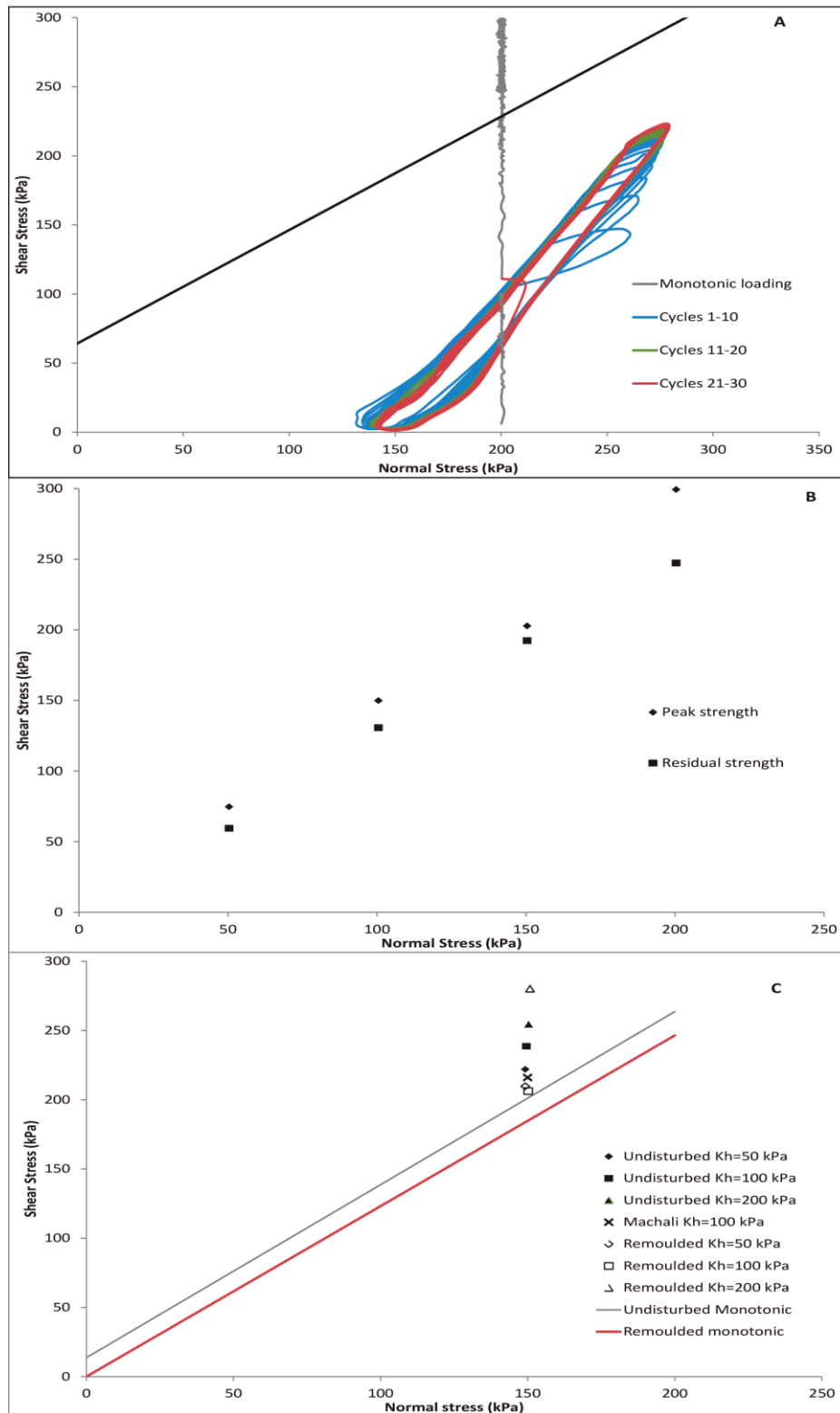
403
 404
 405

Figure 2. Cumulative grain size distribution of the Machalí and Pudahuel samples.



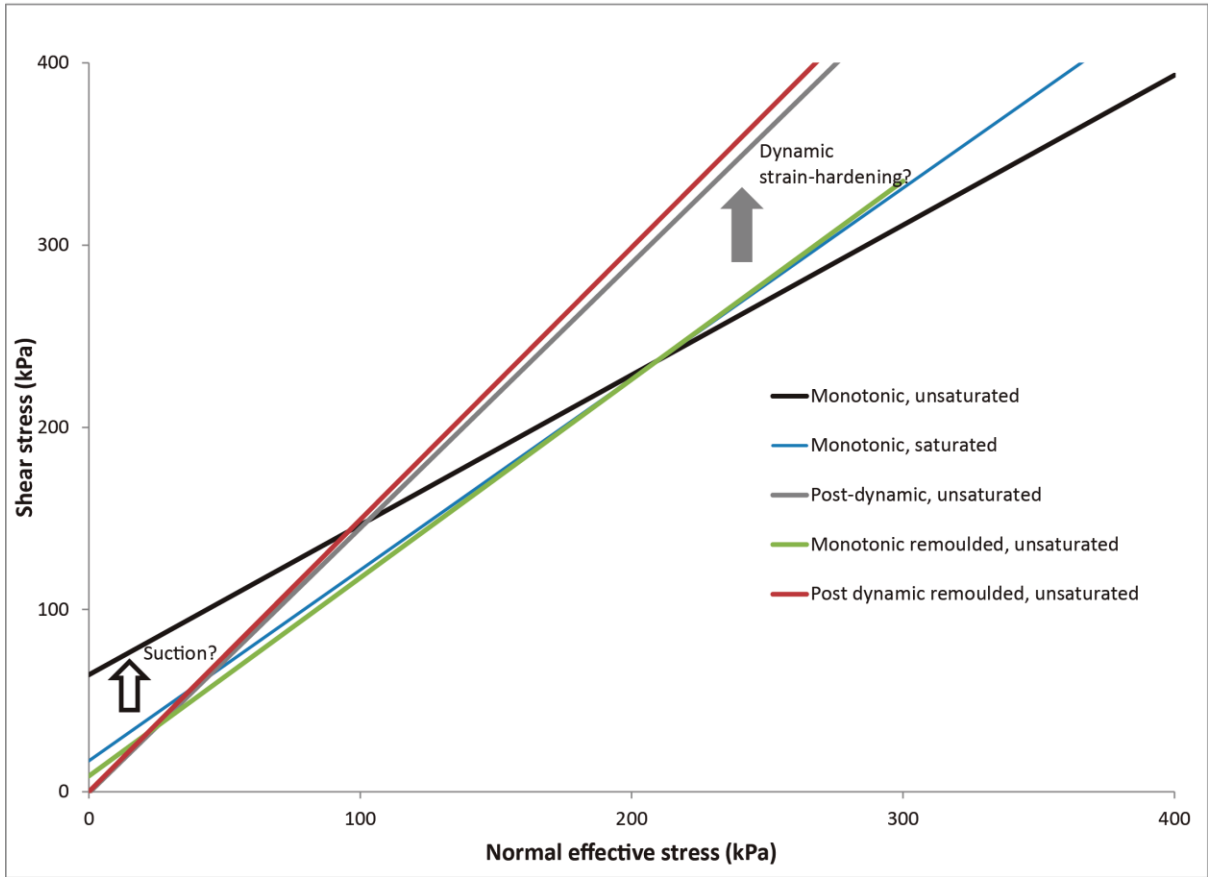
406
 407
 408
 409

Figure 3. Examples of shear stress-shear strain charts of a) monotonic and b) dynamic shear tests on Machalí unsaturated samples at normal stress of 100 kPa.



410

411 Figure 4. Dynamic tests results: a) Example of stress conditions in plot of shear stress vs normal
 412 effective stress during a test on Machalí, undisturbed, unsaturated sample at baseline condition of
 413 200 kPa normal stress. b) Peak and residual strength data for Machalí undisturbed, unsaturated
 414 samples. c) Pudahuel saturated tests post-dynamic peak shear strength for different dynamic
 415 loadings (Kh: horizontal stress amplitude) on both undisturbed and remoulded samples. The
 416 monotonic failure envelopes and one equivalent saturated test of a Machalí undisturbed sample are
 417 also presented for comparison.



418

419 Figure 5. Monotonic and post-dynamic peak strength failure envelopes for the Machalí tests.